

Lawrence Berkeley National Laboratory

Recent Work

Title

CALCULATION OF INTENSITY DISTRIBUTION IN THE VIBRATIONAL STRUCTURE OF ELECTRONIC TRANSITIONS: THE $B^3\Pi_{g+u}-X^1E_{g+g}$ RESONANCE SERIES OF MOLECULAR IODINE

Permalink

<https://escholarship.org/uc/item/2w27m8cv>

Author

Zare, R.N.

Publication Date

1963-10-31

University of California
Ernest O. Lawrence
Radiation Laboratory

TWO-WEEK LOAN COPY

*This is a Library Circulating Copy
which may be borrowed for two weeks.
For a personal retention copy, call
Tech. Info. Division, Ext. 5545*

CALCULATION OF INTENSITY DISTRIBUTION IN
THE VIBRATIONAL STRUCTURE OF ELECTRONIC
TRANSITIONS: THE $B^3\Pi_{o+u} - X^1\Sigma_{o+g}$
RESONANCE SERIES OF MOLECULAR IODINE

Berkeley, California

DISCLAIMER

This document was prepared as an account of work sponsored by the United States Government. While this document is believed to contain correct information, neither the United States Government nor any agency thereof, nor the Regents of the University of California, nor any of their employees, makes any warranty, express or implied, or assumes any legal responsibility for the accuracy, completeness, or usefulness of any information, apparatus, product, or process disclosed, or represents that its use would not infringe privately owned rights. Reference herein to any specific commercial product, process, or service by its trade name, trademark, manufacturer, or otherwise, does not necessarily constitute or imply its endorsement, recommendation, or favoring by the United States Government or any agency thereof, or the Regents of the University of California. The views and opinions of authors expressed herein do not necessarily state or reflect those of the United States Government or any agency thereof or the Regents of the University of California.

UNIVERSITY OF CALIFORNIA
Lawrence Radiation Laboratory
Berkeley, California

AEC Contract No. W-7405-eng-48

CALCULATION OF INTENSITY DISTRIBUTION IN THE VIBRATIONAL
STRUCTURE OF ELECTRONIC TRANSITIONS: THE $B^3\Pi_{o+u} - X^1\Sigma_{o+g}$
RESONANCE SERIES OF MOLECULAR IODINE.

R. N. Zare

October 31, 1963

-i-

CALCULATION OF INTENSITY DISTRIBUTION IN THE VIBRATIONAL
STRUCTURE OF ELECTRONIC TRANSITIONS: THE $B^3\Pi_{o+u} - X^1\Sigma_{o+g}$
RESONANCE SERIES OF MOLECULAR IODINE.

R. N. Zare[†]

Department of Chemistry and Lawrence Radiation
Laboratory, University of California
Berkeley, California

October 31, 1963

Abstract

Franck-Condon overlap integrals have been calculated which predict within experimental error the intensity distribution of the sixty measured lines in the visible fluorescence spectrum of molecular iodine, $B^3\Pi_{o+u} (v' = 15, 16 \text{ or } 26) \rightarrow X^1\Sigma_{o+g} (v'' = 0 \text{ to } 69)$. Rydberg-Klein-Rees potentials were used for both electronic states, and exact vibrational eigenfunctions were obtained by direct numerical solution of the radial Schrödinger equation, including vibration-rotation interaction. The electronic transition moment was assumed to be independent of internuclear distance. Overlap integrals derived in the same way for Morse potentials fail to give even qualitative agreement with experiment for lines with $v'' \gtrsim 10$. Because of the rapid oscillation of the vibrational wavefunctions for high v' and v'' , a shift in the potential of only 0.002 \AA is found to alter appreciably the calculated intensity distribution; thus the agreement obtained provides a very severe test of the RKR potentials and the Franck-Condon principle. The radiative lifetime of the B state has also been calculated from the absolute intensity of a single line and the integrated intensity of the band system, and the results compare favorably with direct lifetime measurements.

* Support received from the U. S. Atomic Energy Commission is gratefully acknowledged.

[†] National Science Foundation Predoctoral Fellow, 1961-63. Present address: Department of Chemistry, Harvard University, Cambridge, Massachusetts.

Franck-Condon factors, computed to as high vibrational quantum numbers v' and v'' as are consistent with spectroscopic data, are of importance for every major molecular band system, since they enter into the calculation of radiative lifetimes, vibrational temperatures, and kinetics of energy transfer, among other applications. Although the Franck-Condon Principle is known to account for the main features of the vibrational intensity distribution in an electronic transition, there have been relatively few quantitative comparisons between theory and experiment. In large part this is due to the difficulty of obtaining reliable intensity data and the labor involved in performing a realistic numerical calculation from theory.

The $B^3\Pi_{o^+u} - X^1\Sigma_{o^+g}$ electronic transition¹ of I_2 , extending from 5000 Å in the visible to about 13,000 Å in the infra-red, is one of the most extensively studied band systems of molecular spectroscopy. The resonance spectrum, which may be excited by any of several atomic lines,² consists of a long series of fluorescence doublets in which the intensity fluctuates irregularly from line to line. The intensity fluctuations arise primarily from the overlap of the wavefunctions characterizing the vibrational levels of the upper and lower electronic states. For high vibrational levels, the wavefunctions are rapidly varying oscillatory functions within the range of the classically allowed motion. The overlap integrals thus depend critically on the phase relation of the initial and final wavefunctions. This specifically non-classical effect has been called "internal diffraction" by Condon.³ For the $v' = 15, 16$ and 26 fluorescence

series of I_2 , for which 60 line intensities have been measured, the internal diffraction patterns are quite complex. For no other molecular system does data exist for transitions at such high vibrational quantum numbers.

Previous calculations of Franck-Condon factors⁴ have made use of a wide variety of analytic potential functions and approximations which allow relatively easy evaluation of the overlap integrals. The results, particularly for the iodine spectrum, have usually been disheartening, except for transitions involving small vibrational quantum numbers ($v', v'' \lesssim 10$). In this paper a calculation based on exact vibrational wavefunctions derived from Rydberg-Klein-Rees potentials is described and the predicted internal diffraction patterns for the iodine resonance series are shown to be at least as accurate as the intensity measurements over the full range of vibrational quantum numbers.

THEORY

The intensity emitted in the line $v', J' \rightarrow v'', J''$ in an electronic transition is given by⁴

$$I_{v''J''}^{v'J'} = (64\pi^4/3) [S_{J''}^{J'} N_{v', J'} / (2J'+1)] c\nu^4 [\int \psi_{v', J'} R_e(r) \psi_{v'', J''} dr]^2 \quad (1)$$

where $S_{J''}^{J'}$ is the rotational line strength given by the Hönl-London⁵ formula, $N_{v', J'}$ is the population of the initial state, ν is the frequency in wave numbers of the line, and ψ_{vJ} is the rotational-vibrational wavefunction characterizing the (v, J) state. The function $R_e(r)$ in Eq. (1) is called the electronic transition moment and is given by

$$\underline{R}_e(r) = \int \psi'_e(q_e, r) M_e(q_e, r) \psi''_e(q_e, r) dq_e \quad (2)$$

in which q_e designates the electronic coordinates, ψ_e an electronic wavefunction, and M_e is that part of the electric dipole transition moment which depends only on the coordinates of the electrons.

No explicit evaluation of Eq. (2) has yet been made for a many-electron molecule. However, it appears reasonable to suppose that $\underline{R}_e(r)$ will be a slowly varying function of r over the small range of r in which the vibrational wavefunctions have appreciable value. By replacing $\underline{R}_e(r)$ in Eq. (2) by an average or effective value, \overline{R}_e , it may be taken outside the integral to give

$$I_{V''J''}^{V'J'} = (64\pi^4/3) [S_{J''}^{J'} N_{V', J'} / (2J'+1)] c v^4 \overline{R}_e^2 (\int \psi_{V', J'} \psi_{V'', J''} dr)^2 \quad (3)$$

where the square of the overlap integral, $(\int \psi_{V', J'} \psi_{V'', J''} dr)^2$, is known as the Franck-Condon factor.

When dealing with each vibrational band as a whole it is customary also to neglect the effects of rotation-vibration interaction. Summation over all lines of the band leads to

$$I^{V'v''} = (64\pi^4/3) N_{V'} c v^4 \overline{R}_e^2 (\int \psi_{V'} \psi_{V''} dr)^2 \quad (4)$$

where now the frequency v characterizes the band as a whole (it is usually taken as the band origin) and the wavefunctions are those for the rotationless ($J=0$) vibrational states. The assumed separation of rotation and vibration is usually a good approximation,⁶ but it should be noted that the calculations

made in this paper do not make this assumption. Instead relative intensities are calculated directly from Eq. (3) by numerical methods.

We proceed now to the straightforward evaluation of Eq. (3). Potential curves for the upper and lower electronic states will be determined from spectroscopic data by the RKR method. These will be used in numerically solving the radial Schrödinger equation for each rotational-vibrational level. The eigenfunctions so obtained will then be used to evaluate the overlap integrals. The final result, with the frequency factor ν^4 taken into account, will be presented as relative intensities for the $v' = 15, 16$ and 26 fluorescence series of the $B \rightarrow X$ transition in iodine. Following some brief remarks on the individual steps in this procedure, a detailed comparison of the calculations with experiment will be made.

CONSTRUCTION OF POTENTIALS

In the Rydberg-Klein-Rees method^{7,8,9} the potential function is derived from experimental vibrational and rotational spectroscopic term values without imposing any assumed analytic form on the potential. The method determines the classical turning points r_+ and r_- for a vibrational level of energy U from the expression

$$r_{\pm}(U) = (f/g + f^2)^{1/2} \pm f \quad (5)$$

where f and g are given by

$$f(U) = \frac{h}{2\pi(2\mu)^{1/2}} \int_0^{I'} [U-E(I,\kappa)]^{-1/2} dI \quad (6)$$

and

$$g(U) = \frac{h}{2\pi(2\mu)^{1/2}} \int_0^{I'} \frac{\partial E}{\partial \kappa} [U-E(I,\kappa)]^{-1/2} dI \quad (7)$$

Here $E(I,\kappa)$ is the sum of the vibrational and rotational energies for any level up to U ; $I = h(v + \frac{1}{2})$ is the action variable arising from the quantization of the radial momentum; $\kappa = J(J+1)h^2/8\pi^2\mu$ comes from the quantization of the angular momentum for a molecule of reduced mass μ ; and $I = I'$ when $E = U$. The variable of integration I is not restricted to discrete values and the integrals in Eqs. (6) and (7) are to be evaluated for $\kappa = 0$ to construct the effective potential function for the non-rotating ($J = 0$) molecule.

The principal difficulty of the RKR method is the accurate evaluation of the integrals appearing in Eqs. (6) and (7) for which the integrand is singular at the upper limit of integration. If $E(I,\kappa)$ is a quadratic function of I and κ , Rees⁹ has shown that Eqs. (6) and (7) can be exactly expressed in closed form. But this restriction on the form of $E(I,\kappa)$ is usually too severe to represent the energy levels over the whole range of the potential. Vanderslice and coworkers¹⁰ have improved upon the Rees treatment by using a series of quadratics over the range of the potential so that a best least squares choice of the spectroscopic parameters ω_1 , ωx_1 , B_1 , α_1 is used for each vibrational level. Recently Jarman¹¹ has used the approach of direct numerical integration of Eqs. (6) and (7) on an IBM 650.

An analytic approximation to $[U-E(I, \kappa)]^{-1/2}$ was employed to overcome the difficulty at the upper limit. Kasper¹² has further investigated this method, discarding entirely the use of an analytic approximation and adding refinements in accuracy made possible through the use of an IBM 7090.

Table I shows a test of the variant RKR procedures of Vanderslice and Kasper. Potential functions were constructed by each method using the same set of observed spectroscopic term values and then each function was employed in turn in a numerical solution of the radial Schrödinger equation. Since the results derived from his program agree with the observed term values within Verma's error of measurement, Kasper's procedure was adopted.

As an additional check on the accuracy of the RKR procedure, the wavefunctions generated by numerical solution of the radial equation were used to compute the expectation values of $\langle 1/r^2 \rangle$ and hence B_v values. For the first thirty vibrational levels tested, the B_v values calculated in this way differed at most by $1 \times 10^{-6} \text{ cm}^{-1}$ from the input B_v values derived from Verma's reported rotational constants. The observed B_v values are not known to this accuracy, but these tests show that the accuracy of the RKR method for I_2 is limited only by the uncertainties in the spectroscopic data. These tests also serve as a useful check on the method for numerical solution of the radial equation.

Table I: Comparison of calculated and observed
 $G(v)$ values for ground state of I_2 .

v	Observed ^a $G(v)$ cm^{-1}	$G(v)_{calc.} - G(v)_{obs.}$ Kasper RKR	$G(v)_{calc.} - G(v)_{obs.}$ Vanderslice RKR
0	107.08	-0.01	3.34
1	320.39	-0.02	3.96
2	532.44	0.01	0.44
3	743.24	0.02	-2.93
4	952.90	-0.02	-3.47
5	1164.40	-0.07	-2.72
6	1368.60	-0.06	-1.25
7	1574.40	0.02	0.72
8	1778.95	-0.01	2.81
9	1982.13	0.01	4.73
10	2184.06	-0.01	6.24
11	2384.74	-0.06	7.03
12	2584.04	-0.02	7.32
13	2782.09	-0.02	7.26
14	2978.82	-0.04	7.23
15	3174.18	-0.03	7.66
16	3368.24	-0.03	8.46
17	3560.97	-0.07	9.50
18	3752.28	-0.06	10.64
19	3942.24	-0.07	11.44
20	4130.71	-0.02	11.82
21	4317.78	-0.01	11.80
22	4503.49	-0.05	11.45
23	4687.70	-0.04	11.12
24	4870.44	-0.01	11.02
25	5051.78	-0.05	11.08
26	5231.63	-0.09	11.38
27	5409.91	-0.07	11.92
28	5586.69	-0.04	12.49
29	5761.92	-0.05	13.00

^aFrom reference 13.

Potential Curve for the X State

Verma¹³ has given a thorough analysis of several ultra-violet resonance series which he had followed nearly to the dissociation limit. From his values of $\Delta G(v)$ and B_v we have constructed the turning points for the first 70 vibrational levels of the ground electronic state. Some of the turning points are given in Table II.

The potential function employed in our calculations is obtained by connecting the turning points with a smooth curve generated by seventh order Lagrangian interpolation.¹⁴ To estimate the potential outside the central region derived from Verma's data, repulsive and attractive segments are smoothly joined to the central portion. In these regions (which, as shown later, do not contribute noticeably in the intensity calculation) the potential is assumed to have the form

$$V_{\text{rep}} = a/r^{12} + b \quad (8)$$

and

$$V_{\text{att}} = a'/r^{b'} \quad (9)$$

where the two constants were determined from the last RKR turning points r_{\pm} for $v'' = 68$ and 69 . Finally the rotational contribution is added to the non-rotating potential $V(r)$ to give the effective radial potential $U(r, J)$

$$U(r, J) = V(r) + \frac{J(J+1)h^2}{8\pi^2\mu r^2}$$

appropriate to the molecule with rotational quantum number J .

Table II. Results of calculations for the potential energy curve^a for the ground state of I₂ (J = 0 rotational state).

Turning Points			Turning Points		
V	r ₋ (Å)	r ₊ (Å)	V	r ₋ (Å)	r ₊ (Å)
0	2.6178	2.7175	33	2.3587	3.2575
1	2.5850	2.7580	35	2.3521	3.2846
2	2.5634	2.7873	37	2.3459	3.3120
3	2.5464	2.8120	39	2.3400	3.3399
4	2.5321	2.8340	41	2.3343	3.3686
5	2.5197	2.8542	43	2.3290	3.3978
6	2.5086	2.8731	45	2.3240	3.4277
7	2.4984	2.8911	47	2.3193	3.4586
9	2.4805	2.9248	49	2.3149	3.4905
11	2.4650	2.9564	51	2.3108	3.5236
13	2.4511	2.9864	53	2.3069	3.5583
15	2.4386	3.0154	55	2.3033	3.5946
17	2.4271	3.0434	57	2.3000	3.6328
19	2.4165	3.0709	59	2.2970	3.6730
21	2.4067	3.0980	61	2.2942	3.7155
23	2.3974	3.1247	63	2.2919	3.7606
25	2.3888	3.1512	65	2.2899	3.8088
27	2.3806	3.1777	67	2.2882	3.8605
29	2.3729	3.2042	68	2.2875	3.8877
31	2.3656	3.2307	69	2.2869	3.9160

^aThe values of the constants in Eqs. (8) and (9) are:

$$a = 5.881 \times 10^8, \quad b = -3.012 \times 10^4; \quad a' = 1.529 \times 10^8, \quad b' = 8.507.$$

Potential Curve for the B State

Although the molecular constants of the ground state have been repeatedly remeasured by different investigators, knowledge of the upper state is not nearly so extensive nor precise. It is based almost solely on the pioneering experimental work of Mecke¹⁵ who first measured the iodine absorption band heads in the region 5000 Å to 7000 Å. By relating Wood's¹⁶ fluorescence series ($v' = 26$) to the iodine absorption spectrum, Loomis¹⁷ re-analysed Mecke's data and established the correct vibrational numbering. The vibrational energy levels can be represented, within the uncertainty of 0.5 cm^{-1} in Mecke's measurements, by

$$G(v) = \omega'_e(v + \frac{1}{2}) - \omega_e x'_e(v + \frac{1}{2})^2 + \omega_e y'_e(v + \frac{1}{2})^3 \quad (11)$$

where we have adopted¹⁸ the values $\omega'_e = 127.35 \text{ cm}^{-1}$, $\omega_e x'_e = 0.76 \text{ cm}^{-1}$ and $\omega_e y'_e = -0.0033 \text{ cm}^{-1}$ for the vibrational parameters.

The rotational analysis, however, which is summarized in Table III, is less satisfactory. Only the first two terms have been determined in the expansion of the rotational constant

$$B_v = B'_e - \alpha'_e(v + \frac{1}{2}) + \gamma'_e(v + \frac{1}{2})^2 + \delta'_e(v + \frac{1}{2})^3 + \dots \quad (12)$$

and the uncertainty in these values is considerable. Mecke studied the individual lines of four bands (4,7), (4,8), (5,7) and (5,8) which lie in the red. From the difference between corresponding lines, Loomis determined the rotational constants from Mecke's data. Loomis also determined the rotational constant of the 29th vibrational level from analysing plates of the iodine absorption spectrum produced by the Mercury green line. From

Table III. Rotational parameters for the B state.

Source	r'_e (Å)	B'_e (cm ⁻¹)	α'_e (cm ⁻¹)
Mecke ^a	3.022	0.02909	0.00015
Loomis ^b	3.016	0.02920	0.00017
Values used ^c	3.022	0.02909	0.00017

^aReference 15. Mecke only determined α'_e . The values given for r'_e and B'_e are based on his α'_e .

^bReference 17. The α'_e shown is a weighted mean of $\alpha'_e = 0.000175$ cm⁻¹ for the difference of the (5,7)-(4,7) band lines and $\alpha'_e = 0.000156$ cm⁻¹ for the (5,8)-(4,8) band lines. Loomis gives $r'_e = 3.01$ Å for the internuclear distance but the value $r'_e = 3.016$ Å, based on his value of B'_e , is commonly cited in the literature in lieu of a more precise measurement. From analysing new plates by Wood and Klingaman of the absorption spectrum, Loomis determined $B'_{29} = 0.023368 \pm 0.000005$ cm⁻¹. He had planned to carry out a more definite analysis of the rotational constants of the B state but this was never published.

^cWith $\gamma'_e = -1.0 \times 10^{-6}$ cm⁻¹ estimated from Loomis' value of B'_{29} .

this value, we have estimated $\gamma'_e = -1.0 \times 10^{-6} \text{ cm}^{-1}$. However, it is doubtful whether Loomis made centrifugal distortion corrections in evaluating B'_{29} . Furthermore, it is possible that a δ'_e term would be required to represent the B_v values through the 29th level, and δ'_e cannot be calculated without additional data.

If the rotational constants determined by Loomis are used to obtain the upper state potential, the calculated intensity distribution gives reasonable agreement¹⁹ with experiment for only the lower v'' members (up to about $v'' = 18$). Instead we have used the values of B'_e , α'_e and γ'_e given in Table III to construct the turning points for the upper state shown in Table IV. The only change from Loomis is in the value of B'_e , which has been adjusted to shift the upper state potential curve to the left by about 0.006 \AA . This change could be achieved equally as well in a number of other ways for these high vibrational levels, such as small corrections in values of α'_e or γ'_e and the inclusion of a δ'_e term. But these rotational constants lie within the bounds of the experimental uncertainty ($r'_e = 3.016 \pm 0.010 \text{ \AA}$) and give excellent agreement with the observed intensity distribution.

The errors introduced into the RKR turning points by inaccurate rotational constants are rather small for the lower vibrational levels but rapidly build up. For the higher vibrational levels, the potential energy function is quite sensitive to the rotational constants. The width of the potential curve $r_+ - r_- = 2f(V)$, given by Eq. (6), depends on the vibrational constants alone. However, the slant of the central axis of the potential curve, i.e., how much each pair of turning points are

Table IV. Results of calculations for the potential energy curve^a of the B state of I₂ (J = 0 rotational state).

Turning Points			Turning Points		
V	r ₋ (Å)	r ₊ (Å)	V	r ₋ (Å)	r ₊ (Å)
0	2.9609	3.0904	16	2.7503	3.5701
1	2.9203	3.1457	18	2.7393	3.6206
2	2.8942	3.1868	20	2.7292	3.6717
3	2.8741	3.2222	22	2.7199	3.7239
4	2.8575	3.2543	24	2.7111	3.7774
5	2.8432	3.2843	26	2.7026	3.8326
6	2.8307	3.3129	28	2.6944	3.8898
8	2.8092	3.3672	30	2.6863	3.9494
10	2.7913	3.4192	32	2.6781	4.0118
12	2.7759	3.4699	34	2.6697	4.0776
14	2.7624	3.5201	35	2.6654	4.1119

^aThe values of the constants in Eqs. (8) and (9) are:
 $a = 4.117 \times 10^8$, $b = -4.293 \times 10^3$; $a' = -1.215 \times 10^8$, $b' = 6.590$.

displaced to the left or right of r_e , is mainly determined by the rotational constants. For high vibrational levels, γ_e , for example, plays a significant role as can be seen from Table V, which gives the turning points for the $v' = 26$ level for different values of γ_e . Table V shows that the turning points are shifted linearly to the right with increasingly negative γ_e . A 15% error in γ_e will produce an uncertainty of $\pm 0.005 \text{ \AA}$ in the turning points of the $v' = 26$ level. Such a shift will be shown to alter markedly the intensity pattern. The same error in $\omega_e y_e'$ would be unnoticed. Consequently accurate rotational constants are of importance for relative intensity calculations.

COMPUTATION OF THE VIBRATIONAL WAVEFUNCTIONS

Once the potential is constructed, the vibrational wavefunctions appropriate to this potential are obtained by solving the radial Schrödinger equation. Recently Cooley²⁰ has described a rapid and accurate numerical method for this purpose which has been reviewed in detail elsewhere.²¹ Briefly, the one-dimensional second order differential equation

$$\frac{d^2 \psi_{vJ}}{dr^2} + [E_{vJ} - U(r, J)] \psi_{vJ} = 0 \quad (13)$$

is replaced by an equivalent finite difference equation. This is iteratively solved for the eigenvalue E_{vJ} of the total energy and the wavefunction ψ_{vJ} by employing a Numerov²² method of integration, together with a second-order iteration-variation procedure due to Löwdin.²³ In Eq. (13) $U(r, J)$ is the effective

Table V. Sensitivity of turning points
to γ_e' for $v' = 26$.

γ_e' (cm^{-1})	r_+ (\AA)	r_- (\AA)
-1.0×10^{-6}	3.8326	2.7026
-1.2	3.8374	2.7074
-1.4	3.8422	2.7122
-1.6	3.8470	2.7270

potential function of Eq. (10), including the rotational contribution, length is measured in Bohr radii a_0 , and the unit of energy is equivalent to $h N_0 / 8\pi^2 c a_0^2 \mu = 0.948844 \text{ cm}^{-1}$, where N_0 is Avogadro's number (physical scale) and μ is the reduced mass in Aston units.

Cooley has made available a SHARE program embodying these procedures for the IBM 704. This has been made compatible with the IBM 7090 and some useful modifications have been added.²¹ Additional tests of this program have been conducted by Cashion²⁴ who finds that it requires 0.4 seconds to compute the eigenfunction at 1000 points and to correct the trial eigenvalue for the next iteration. Furthermore, relatively few (often less than four) iterations are required in order to obtain eight-figure constancy in the eigenvalue, even for an initial trial energy several percent in error.

The evaluation of the overlap integrals is accomplished by Simpson's rule between the limits 1.500 Å to 6.450 Å in steps of 0.0025 Å. This method of integration as well as the reliability of the wavefunctions were checked by halving the step size, changing the limits of integration and comparing the computed expectation value of $\langle 1/r^2 \rangle$ with the exact expression for the Morse potential. These tests show that integrals of these numerical wavefunctions are accurate beyond five significant figures.

Figure 1 shows the vibrational wavefunctions obtained by this method for the $v' = 26$ level of the upper state and the $v'' = 10$ and 25 levels of the ground state of I_2 . The sensitivity of the overlap integrals to the relative location of the potential

curves may be illustrated with these wavefunctions. As v'' increases, the widening of the potential makes room for new loops in the wavefunction at about the same rate as they appear; thus for $v'' \approx 20$, the length of a loop remains almost constant at about 0.03 \AA . The corresponding length for the $v' = 26$ level of the upper state is 0.04 \AA . The value of the overlap integral for $v' = 26$, $v'' = 25$ will be determined almost entirely by the narrow interval ΔX , which contains about 15 nodes of the upper state and 17 nodes of the lower. For the two wavefunctions to be less than a quarter wavelength out of step with each other, the wavefunctions and hence the turning points of the potential curves must be known to better than 0.01 \AA .

COMPARISON OF CALCULATED AND OBSERVED INTENSITY DISTRIBUTION

Relative intensity measurements for the B-X transition of I_2 are available for only three v'' band progressions: the $v' = 15$ and $v' = 16$ fluorescence series excited by the Sodium D lines; and the $v' = 26$ fluorescence series excited by the Mercury green line. If the light source is highly monochromatic, it produces resonant absorption into a definite rotational-vibrational level of the B state. The subsequent fluorescence to the different rotational-vibrational levels of the ground state produces a long series of closely spaced P and R doublets.

During the first quarter of the century R. W. Wood¹⁶ carried out an extensive study of the $v' = 26$, $J' = 34$ series, which he was able to measure out to the 28th member. W. Lenz²⁵ examined

a reproduction of Wood's plates and roughly estimated the relative intensity of the first 20 members. O. Oldenberg,²⁶ using specially sensitized plates, extended the observed series to the 38th member at 8835 Å, the upper limit of his plate sensitivity. Unfortunately, Oldenberg's measurements do not overlap with the portion of the series analyzed by Lenz. Also, because of intensity limitations, Oldenberg had to use a broad green line and low dispersion and consequently his measurements include some contribution from transitions which originate in excited levels other than $v' = 26$, $J' = 34$. Neither Lenz nor Oldenberg appear to have corrected for variation of film sensitivity with wavelength, and their intensity data are visual estimates of plate blackening. Recently, Arnot and McDowell²⁷ have rephotographed the first 19 members of the series, using narrow line excitation, and have determined the peak heights from densitometer tracings. Also, Rank²⁸ has remeasured the position of the $v'' = 1$ to 13 and $v'' = 29$ to 39 members; although Rank did not make intensity measurements, the lines missing from his list serve to identify transitions of negligible intensity.

Table VI compares the experimental results for the $v' = 26$ fluorescence series with those calculated from both the RKR and the Morse potentials. Despite the considerable discrepancies and uncertainties in the experimental intensity estimates, the location of the maxima and minima in the internal diffraction pattern is well established, and thus offers a severe test of the calculated intensities. If anything within 50% is regarded as within the bounds of experimental error, both the RKR and Morse calculations

Table VI. Calculated and observed relative intensities for the
 $v' = 26, J' = 34$ fluorescence series of I_2 .

v''	Observed Lenz ^a	Observed Arnot and McDowell	Calculated RKR ^b	Calculated Morse ^b	v''	Observed Oldenberg	Calculated RKR ^b	Calculated Morse ^b
0	10	10.0	10.00	7.84	20	e	1.41	0.10
1	9	3.7	9.59	10.00	21	0 ^f	0.01	1.63
2	1 ^c	0.0	0.04	0.28	22	9	1.36	0.01
3	9	3.2	5.10	4.82	23	2	0.20	1.54
4	3	0.9	2.16	2.53	24	3	0.82	0.02
5	8 ^c	? ^d	1.33	1.43	25	9	0.72	1.38
6	8	2.2	3.55	3.61	26	0	0.21	0.10
7	2 ^c	0.2	0.02	0.15	27	10	1.06	1.18
8	9	2.5	3.16	3.48	28	1	0.00	0.24
9	0 ^c	0.1	0.45	0.05	29	9	0.92	0.94
10	8	1.9	1.82	2.79	30	9	0.28	0.41
11	3	1.0	1.46	0.42	31	0 ^c	0.42	0.69
12	2 ^c	0.6	0.56	1.97	32	10	0.70	0.60
13	7	1.7	2.10	0.88	33	1 ^c	0.04	0.44
14	0	0.0	0.01	1.24	34	9	0.81	0.79
15	7	1.7	1.97	1.26	35	5	0.09	0.22
16	0	0.2	0.26	0.69	36	2	0.51	0.94
17	2	1.2	1.23	1.51	37	2	0.44	0.06
18	1	1.0	0.92	0.32	38	c	0.11	1.02
19	0 ^f	...	0.41	1.63	39	e	0.67	0.00

(footnotes follow)

Table VI. Footnotes

^aNote that the normalization used by Lenz is not related to that of Oldenberg.

^bBoth the P(35) and R(35) doublet intensities were evaluated from Eq. (3). Since they do not differ from each other by more than 2%, their average normalized to the 26'-0" transition is reported above. The RKR potentials used are given in Tables II and IV; the Morse potential parameters are $r_e'' = 2.6666 \text{ \AA}$, $\omega_e'' = 214.52 \text{ cm}^{-1}$ and $D_e'' = 12554.6 \text{ cm}^{-1}$ for the X state and $r_e' = 3.022 \text{ \AA}$, $\omega_e' = 127.35 \text{ cm}^{-1}$ and $D_e' = 4507.0 \text{ cm}^{-1}$ for the B state.

^cIndicated as very weak by Rank, reference 28.

^dThe observation of this line is made difficult by overlapping with the yellow Mercury line at 5790 \AA .

^eThe line has been observed but no intensity estimate has been made.

^fIndicated as very weak by Wood, reference 16.

are satisfactory up to $v'' = 10$. At higher v'' the RKR results continue to follow the experimental intensity fluctuations whereas above $v'' = 11$ the Morse results fall "in and out-of-step." Various choices of the Morse parameters were tried with similar results.²⁹ Figure 2 shows an example in which r'_e has been adjusted, within the uncertainty indicated in Table III; again the Morse results fall "out of step" by $v'' = 11$. The most satisfactory procedure, which gave results that paralleled the RKR results up to $v'' = 15$, was obtained by adjusting the Morse potential for the B state to fit the RKR potential near the $v' = 26$ level.³⁰

The sensitivity of the Franck-Condon factors to changes in the potential function is illustrated in Fig. 3, which compares several calculated intensity patterns obtained by displacing the RKR potential curve for the B state by increments of $\Delta(r'_e - r''_e) = 0.002 \text{ \AA}$, with the ground state curve fixed in position. Only when the relative location of the potential curves is correct within displacements of this order will the calculated intensity pattern match the observed one over a wide range of vibrational quantum numbers.

Brown has recently carried out a very careful study of the first ten members of the $v' = 15$, P(114) and $v' = 16$, P(45) fluorescence series.³¹ His results are compared with the RKR calculations in Tables VII and VIII. Brown measured the intensities photometrically and made corrections for the variation in photomultiplier response with wavelength. For the measurements considered in Table VII, he estimated the

experimental uncertainty as $\pm 30\%$ for $v'' > 3$, and even higher for the lines with $v'' < 3$, which are subject to self-absorption. Nevertheless, the agreement between the calculated and experimental intensities is quite satisfactory. In a second set of measurements at tenfold lower pressure of iodine (30 microns), Brown evaluated the self-absorption corrections experimentally and determined intensity ratios for a few lines with an estimated accuracy of $\pm 10\%$. These ratios are in excellent agreement with the calculated values, as shown in Table VIII.

Thus, we find in Tables VI-VIII that, within the experimental uncertainty present in the spectroscopic constants and the relative intensity measurements, the relative intensity pattern calculated from RKR potentials matches the experimental intensity for the sixty lines of the B-X transitions measured to date. It is also found that 7 additional lines: $(v', v'') = (26, 2), (26, 7), (26, 9), (26, 12), (26, 31), (26, 33),$ and $(26, 38)$, indicated as missing by Rank are indeed predicted to have negligible intensity.

Table IX gives the calculated relative intensities for all transitions of appreciable intensity in the $v' = 15, 16$ and 26 fluorescence series. Table IX shows that the primary means of depopulating the (v', J') level of the upper state is by transitions to the first few vibrational levels of the ground state. However, the fluorescence series extends far into the infra-red with appreciable intensity, and a weaker secondary maxima in the intensity pattern is predicted to occur around $v'' = 51$ and 52 for the $v' = 15$ and $v' = 16$ fluorescence series and around

Table VII. Calculated and observed relative intensities for the $v' = 15$ and $v' = 16$ fluorescence series of I_2 .

v''	$v' = 15$ P(144) Series		$v' = 16$ P(45) Series	
	Brown	Calculated RKR	Brown ^c	Calculated RKR
0	a	0.9	0.8	1.3
1	a	5.0	4.0	6.2
2	10.0	10.0	b	10.0
3	9.2	7.6	5.0	4.9
4	2.4	0.7	0.0	0.0
5	2.9	2.1	3.8	4.0
6	6.7	5.3	4.0	3.8
7	2.4	1.2	0.0	0.0
8	1.0	1.1	2.5	3.0
9	3.7	3.9	2.3	2.6

^aNot reported.

^bMasked by scattered sodium light.

^cScaled arbitrarily.

Table VIII. Comparison of intensity ratios.

Line Intensity Ratio	Experimental Brown	Calculated RKR
(15-3)/(15-2)	0.77 ± 0.15	0.76
(16-0)/(16-1)	0.22 ± 0.04	0.21
(16-3)/(16-1)	0.76 ± 0.15	0.79

Table IX. Summary of calculated relative intensities for the $v' = 15, 16$ and 26 fluorescence series. All intensities have been scaled to ten. The calculated values reported for the $v' = 26$ progression are an average of the P(35) and R(33) doublet intensities.

v''	$v' = 15$ P(114)	$v' = 16$ P(45)	$v' = 26$ J'=34	v''	$v' = 15$ P(114)	$v' = 16$ P(45)	$v' = 26$ J'=34	v''	$v' = 15$ P(114)	$v' = 16$ P(45)	$v' = 26$ J'=34
0	0.89	1.31	10.00	24	1.01	0.04	0.82	48	0.03	0.68	0.18
1	4.96	6.23	9.59	25	0.04	1.31	0.72	49	0.83	0.03	0.47
2	10.00	10.00	0.04	26	1.33	0.68	0.21	50	1.69	0.36	0.00
3	7.58	4.88	5.10	27	0.80	0.13	1.06	51	1.69	1.29	0.47
4	0.68	0.01	2.16	28	0.06	1.23	0.00	52	1.08	1.64	0.17
5	2.09	4.00	1.33	29	1.20	0.46	0.92	53	0.47	1.22	0.19
6	5.31	3.83	3.55	30	0.71	0.19	0.28	54	0.14	0.59	0.46
7	1.15	0.01	0.02	31	0.05	1.12	0.42	55	0.03	0.20	0.00
8	1.08	2.97	3.16	32	1.05	0.35	0.70	56	a	0.05	0.49
9	3.93	2.55	0.45	33	0.71	0.20	0.04	57		0.01	0.20
10	0.80	0.04	1.82	34	0.01	1.02	0.81	58		a	0.18
11	1.05	2.76	1.46	35	0.87	0.33	0.09	59			0.60
12	3.10	1.45	0.56	36	0.80	0.15	0.51	60			0.01
13	0.38	0.30	2.10	37	0.01	0.93	0.44	61			0.57
14	1.22	2.52	0.01	38	0.63	0.40	0.11	62			0.62
15	2.42	0.63	1.97	39	0.94	0.07	0.67	63			0.01
16	0.11	0.71	0.26	40	0.11	0.82	0.19	64			1.22
17	1.39	2.08	1.23	41	0.31	0.56	0.51	65			2.04
18	1.83	0.16	0.92	42	1.01	0.00	0.28	66			1.13
19	0.01	1.08	0.41	43	0.48	0.62	0.15	67			0.25
20	1.46	1.54	1.41	44	0.01	0.81	0.54	68			0.02
21	1.35	0.00	0.01	45	0.73	0.00	0.10	69			a
22	0.01	1.28	1.36	46	1.08	0.25	0.49				
23	1.43	1.04	0.20	47	0.36	0.95	0.20				

^a Negligible intensities for higher members of progression.

$v'' = 65$ for the $v' = 26$ fluorescence series. A calculation of the radiative lifetime of the $v' = 15, 16$ and 26 level based on the relative intensities given in Table VII is presented in the Appendix.

DISCUSSION

The Rydberg-Klein-Rees potential functions, properly evaluated, have been shown to reproduce accurately the observed spectroscopic term values (Table I) and to give Franck-Condon overlap integrals which, within experimental error, account for the observed internal diffraction pattern of the B-X transition of I_2 (Tables VI-VIII) over a wide range of vibrational quantum numbers. The agreement found for this extreme case encourages the application of these exact numerical methods to other molecular band systems.³² Unfortunately, for many examples of interest, the available spectroscopic data is not sufficient to enable accurate RKR potentials to be constructed, especially for excited electronic states. In particular, it is necessary to have accurate rotational constants in order to determine the relative position of the potential curves as the overlap integrals are very sensitive to this (Table V and Fig. 3). In the absence of the requisite data, recourse must be had to analytic approximations, and it is reassuring to find that overlap integrals computed from Morse potentials closely simulate the RKR results for low vibrational quantum numbers.

Since our calculations, based on Eqs. (3) and (13), have taken into account the centrifugal distortion of the potential

due to rotation, we may examine the contribution from this effect, which has been ignored in previous calculations of Franck-Condon factors. It is found that the use of Eq. (4), which neglects vibration-rotation interaction, gives intensities in error by about $\pm 10\%$ for $J' = 34$, and by $\pm 20\%$ for $J' = 113$; furthermore, the error does not show a systematic trend but varies irregularly from line to line. If the rotational contribution is neglected, a systematic error is introduced into the calculated lifetime for the upper state (see the Appendix), although an error of 10-20% is well within the experimental uncertainty of most intensity measurements.

Equation (3), on which this analysis is based, assumes the Born-Oppenheimer approximation for the separability of electronic and nuclear motion, and the adequacy of a constant electronic transition moment \bar{R}_e independent of r over the entire v'' progression of a fluorescence series. The validity of this last assumption is a matter of some importance since the sum rules of molecular spectroscopy, from which (among other consequences) radiative lifetimes are deduced, strictly obtain only for a constant average \bar{R}_e .

Recently it has been possible to calculate exactly the variation of $R_e(r)$ with r for the one-electron molecules H_2^+ by Bates et al.³³ and HeH^{++} by Arthurs et al.³⁴ Both these molecules have only one bound state ($1s\sigma$ for H_2^+ and $2p\sigma$ for HeH^{++}) and the strength of transitions to repulsive electronic states have been determined over a wide range of r .

For H_2^+ the calculations refer to strongly allowed transitions and the oscillator strength [proportional to $R_e^2(r)$] is found to be quite constant, varying by no more than 15% from its mean value over a range of 1 Å centered about the r_e of the bound state. A similar calculation for HeH^{++} likewise gives a slowly varying oscillator strength for the strongly allowed transitions but a rapidly varying oscillator strength which changes by as much as a factor of ten for the weakly allowed charge transfer transitions. It is not clear whether these results can be generalized for many-electron molecules.

Mulliken³⁵ has suggested a relatively rapid variation of $R_e(r)$ for the charge transfer type B-X transitions of the halogens, since it is forbidden for separated atoms and enhanced by case c coupling in the united atom limit. Using approximate calculations for chlorine and bromine reported by Mulliken's laboratory, Stafford³⁶ has estimated a change in $R_e^2(r)$ by no more than a factor of two to four over the extremes of the iodine absorption spectrum. It may be noted, however, that the same molecular orbital treatment applied to H_2^+ or HeH^{++} leads to predicted variation of $R_e(r)$ which are considerably too rapid.^{33,34}

Fraser³⁷ has suggested that observed intensities be used to determine the functional form of $R_e(r)$, by means of "the r-centroid method." This employs the approximation³⁸ [which is exact for a linear variation of $R_e(r)$]:

$$\int \psi_{V'} R_e(r) \psi_{V''} dr = R_e(\bar{r}_{V',V''}) \int \psi_{V'} \psi_{V''} dr \quad (14)$$

where $\bar{r}_{v',v''}$, called the r-centroid, is a weighted value of r encountered in the $v' \rightarrow v''$ transition, and is defined by

$$\bar{r}_{v',v''} = \int \psi_{v'} r \psi_{v''} dr / \int \psi_{v'} \psi_{v''} dr. \quad (15)$$

From Eq. (4), observed band intensities may be used to determine the variation of $R_e(\bar{r}_{v',v''})$ with $\bar{r}_{v',v''}$ from the relation

$$R_e^2(\bar{r}_{v',v''}) = I^{v',v''} / (N_{v',v''}^4 [\int \psi_{v'} \psi_{v''} dr]^2) \quad (16)$$

using calculated values of the r-centroids and Franck-Condon factors involved in each transition.

The r-centroid method has been applied to many molecular band systems.⁴ Since it ascribes all discrepancies between the calculated and observed intensities to the variation of $R_e(\bar{r}_{v',v''})$ with $\bar{r}_{v',v''}$, it should be emphasized that the results can only be valid if both the experimental intensity and the calculated Franck-Condon factors are highly accurate. For I_2 the uncertainties are such that there is no possibility to assess the variation of the electronic transition moment with inter-nuclear distance.

APPENDIX

Radiative Lifetime for I₂ Fluorescence

The radiative lifetime of a rotational-vibrational level (v', J') of the upper state is defined as

$$\tau_{v', J'} = \left[\sum_{v'', J''} A_{v'' J''}^{v' J'} \right]^{-1} \quad (17)$$

where $A_{v'' J''}^{v' J'}$ is the probability of spontaneous emission per second from the level (v', J') to the level (v'', J'') and the sum is taken over all levels of the ground state for which the transition is allowed. Once relative intensities are known, the radiative lifetime may be calculated from measurement of either the absolute intensity of a single line or the integrated intensity of the entire band system.

The fluorescence intensity of a spectral line (in units of energy emitted per second) is proportional to the transition probability of spontaneous emission $A_{v'' J''}^{v' J'}$ and the frequency of the transition $\nu_{v'' J''}^{v' J'}$ (in wave numbers). If relative intensities are available and $A_{v'' J''}^{v' J'}$ has been determined by an absolute intensity measurement for the $v' J' \rightarrow v^* J^*$ transition, the lifetime of the (v', J') level is simply given by

$$1/\tau_{v', J'} = A_{v^* J^*}^{v' J'} \frac{\sum_{v'' J''} \left[I_{v'' J''}^{v' J'} / \nu_{v'' J''}^{v' J'} \right]}{\left[I_{v^* J^*}^{v' J'} / \nu_{v^* J^*}^{v' J'} \right]}, \quad (18)$$

provided that certain vibrational and rotational sum rules of molecular spectroscopy are applicable.³⁹ Using the relative

intensities listed in Table IX and Einstein A coefficients reported by various workers, we have calculated lifetimes for the $v' = 15, 16,$ and 26 vibrational levels and the results are given in Table X.

Total band absorption measurements provide another means of estimating the radiative lifetime, although the theoretical basis of this formulation is more open to question. It may be shown⁴⁰ that the absorption data can be related to the lifetime by the following equation

$$1/\tau = 2.880 \times 10^{-9} \langle v_f^{-3} \rangle_{av}^{-1} \int \epsilon d \ln v_a. \quad (19)$$

where ϵ is the decadic molar extinction coefficient and v_f and v_a are the frequencies of fluorescence and absorption in wave numbers. The mean fluorescence frequency factor appropriate to the entire band system is obtained from the expression

$$\langle v_f^{-3} \rangle_{av}^{-1} = \sum_{v''J''} \frac{[I_{v''J''}^{v'J'} / (v_{v''J''}^{v'J'})^4]}{[I_{v''J''}^{v'J'} / v_{v''J''}^{v'J'}]} \quad (20)$$

by use of the relative intensity data found in Table IX. For the $v' = 26$ level the calculated mean fluorescence wavelength is 8867 \AA . This result is 15% higher than the estimate given in reference 43. Lifetimes based on the 8867 \AA value and the extinction coefficient measurements of Rabinowitch and Wood⁴¹ for a pressure broadened spectrum and those of Sulzer and Wieland⁴² on superheated I_2 vapor are also given in Table X.

Recently the lifetime of the $v' = 26$ level has been directly measured by Brewer, Berg, and Rosenblatt⁴³ who obtained a value

of $(7.2 \pm 1.0) \times 10^{-7}$ seconds by using a phase fluorometer. It is seen that this reported lifetime lies between the lifetime calculated from the absolute line intensity and that from the integrated band absorption. In view of the large uncertainties possible in absolute intensity measurements and the approximations made in Eqs. (18) and (19), the calculated lifetimes are in satisfactory agreement with the direct observation.

The lifetime may be related to the electronic transition moment by

$$1/\tau_{v'J'} = (64\pi^4/3) h \bar{R}_e^2 \sum_{v''J''} (v_{v''J''}^{v'J'})^3 \quad (21)$$

where the lifetime of the $(v'J')$ level of the upper state is seen to depend on v' (and very slightly on J') only through the cube of the frequency factor. Consequently one would expect the lifetime for the $v' = 15$ and $v' = 16$ levels to be about 20% greater than the lifetime of the $v' = 26$ level, provided $R_e(r)$ does not vary appreciably from transition to transition. This trend to longer lifetimes is qualitatively borne out by Table X.

No direct lifetimes for the $v' = 15$ or $v' = 16$ levels have yet been determined. The source of the discrepancy between lifetimes calculated from absolute line intensity or band absorption data, as well as the possibility of assessing the validity of the rotational and vibrational sum rules must await the further comparison of calculated lifetimes, based on accurate Franck-Condon factors, and observed lifetimes, determined by direct measurements.

Table X. Calculated radiative lifetimes for I₂ fluorescence.

Absolute Line Intensity				Integrated Band Intensity	
v'J'	v''J''	$A_{v''J'' \rightarrow v'J'} \times 10^5 (\text{sec}^{-1})$	$\tau_{v'J'} \times 10^{-7} (\text{sec})$	$\int \epsilon d \ln v_a$	$\tau_{v'} \times 10^{-7} (\text{sec})$
15,113	3,114	2.8 ± 0.3^a	2.9 ± 0.3	155 ± 30^c	18 ± 4
16,44	3,45	1.0 ± 0.2^a	5.6 ± 1.1	134 ± 20^d	15 ± 2
26,34	3,33 or 35	2.0 ± 1.6^b	2.9 ± 2.4		

^aFrom reference 31.

^bFrom reference 44.

^cFrom reference 41.

^dFrom reference 42.

ACKNOWLEDGEMENTS

It is a pleasure to thank Professor D. R. Herschbach for suggesting this problem and for many stimulating discussions. I am also deeply indebted to Mr. J. V. V. Kasper and to Dr. J. K. Cashion for their assistance and suggestions. I have enjoyed discussions of this work with Dr. R. A. Berg, Dr. Gerd Rosenblatt and Professor Leo Brewer, and correspondence with Drs. R. W. Nicholls, R. D. Verma, and A. L. G. Rees.

References

1. Our notation for the electronic states emphasizes the strong Hund's case c coupling for I_2 and is consistent with reference 43.
2. P. Pringsheim, Fluorescence and Phosphorescence, Interscience Publishers (New York), 1949.
3. E. U. Condon, Am. J. Phys. 15, 365 (1947). As Condon has remarked, "internal diffraction is just as real and forceful a proof for the wave nature of nuclear motion as any of the basic external diffraction experiments....which also are determined by a phase relation between initial and final wavefunctions."
4. An extensive review is given by R. W. Nicholls and A. L. Stewart in "Allowed Transitions" Chapter 2 of Atomic and Molecular Processes, (D. R. Bates, Ed.), Academic Press, New York, 1962.
5. H. Könl and F. London, Z. Physik 33, 803 (1925). These factors are tabulated in reference 39, p. 208.
6. T. C. James, "Studies of Rotation-Vibration Interaction," thesis (Harvard University, 1960).
7. R. Rydberg, Ann. Physik 73, 376 (1931).
8. O. Klein, Z. Physik 76, 226 (1932).
9. A. L. G. Rees, Proc. Phys. Soc. A59, 998 (1947).
10. References to previous work may be found in the review article: D. Steele, E. R. Lippincott and J. T. Vanderslice, Rev. Mod. Phys. 34, 239 (1962).
11. W. R. Jarman, Sci. Rept. No. 1 and 2, Grant No. AF-AFOSR-61-88, Department of Physics, University of Western Ontario, Canada (1961).

References (Continued)

12. J. V. V. Kasper, (Private communication) University of California, Berkeley. The author wishes to thank Mr. Kasper for making these programs available to him.
13. R. D. Verma, J. Chem. Phys. 32, 738 (1960). Kasper has confirmed by private communication with Verma that a 5 cm^{-1} error was made in the zero point energy used in Table VII of his paper. Since Verma calculated the turning points for the ground state from his $\Delta G(v)$ rather than $G(v)$ data, the only correction to his Table VII is to raise all $G(v)$ values 5 cm^{-1} .
14. Other forms of interpolation proved unsatisfactory. This method is able to interpolate points on a Morse curve with considerable accuracy.
15. R. Mecke, Ann. Physik 71, 104 (1923).
16. R. W. Wood, Phil. Mag. 21, 236 (1911).
17. F. W. Loomis, Phys. Rev. 29, 112 (1927).
18. Lois Mathieson and A. L. G. Rees, J. Chem. Phys. 25, 753 (1956).
19. R. N. Zare, Inorganic Materials Research Division Annual Report, 1962, University of California, Berkeley, U. S. Atomic Energy Commission UCRL-10706, p. 84. A similar undertaking for the IBM 650 has been reported by W. R. Jarman, Can. J. Phys. 41, 414 (1963).
20. J. W. Cooley, Math. of Computation, XV, 363 (1961).
21. R. N. Zare and J. K. Cashion, University of California Radiation Laboratory UCRL-10881 (July 1963).
22. B. Numerov, Publ. Observatoire Central Astroph. Russ. 2, 188 (1933).
23. P. O. Löwdin, J. Molecular Spec. 10, 12 (1963).

References (Continued)

24. J. K. Cashion, J. Chem. Phys. 39, 1872 (1963).
25. W. Lenz, Z. Physik 25, 299 (1924).
26. O. Oldenberg, Z. Physik 45, 451 (1927).
27. The relative intensities cited are quoted in reference 36. The data was obtained as part of the work: C. Arnot and C. A. McDowell, Can. J. Chem. 36, 114, 1322 (1958).
28. D. H. Rank, J. Opt. Soc. Am. 36, 239 (1946).
29. In preliminary calculations on other molecular spectra, further comparisons between the Morse and RKR potentials have been made. It is found that even when $r'_e - r''_e$ is small, overlap integrals derived from the Morse potential are only satisfactory for small v' and v'' . Since the α_e given by the Morse potential is systematically too large [see V. P. Varshni, Rev. Mod. Phys. 29, 664 (1957)], the slant of the central axis of the potential is incorrect, and the overlap integrals are sensitive to this as illustrated in the discussion of Table V.
30. The adjusted Morse parameters are: $r'_e = 3.016 \text{ \AA}$, $\omega'_e = 129.834 \text{ cm}^{-1}$ and $\omega'_e x'_e = 0.834 \text{ cm}^{-1}$. This adjusted potential was employed in the overlap integral calculations reported by R. W. Nicholls, J. Chem. Phys. 38, 1029 (1963).
31. R. L. Brown, Thesis, Harvard University, Cambridge, Massachusetts, 1962.
32. All computer programs described in this paper have been documented in R. N. Zare, University of California Radiation Laboratory Report, UCRL-10925 (1963).
33. D. R. Bates, R. T. S. Darling, S. C. Hawe and A. L. Stewart, Proc. Phys. Soc. A66, 1124 (1953). See also, D. R. Bates, J. Chem. Phys. 14, 1122 (1951).

References (Continued)

34. A. M. Arthurs and J. Hyslop, Proc. Phys. Soc. A70, 489, 849 (1957); A. M. Arthurs, R. A. B. Bond and J. Hyslop, Ibid. 617 (1957).
35. R. S. Mulliken and C. A. Riecke, Repts. Prog. Phys. 8, 231 (1941).
36. F. E. Stafford, Thesis, University of California Radiation Laboratory Report, UCRL-8854 (1959).
37. P. A. Fraser, Can. J. Phys. 32, 516 (1954).
38. Once accurate wavefunctions are available, the r-centroid method may be made exact. The electronic transition moment $R_e(r)$ may be expanded about $z = (r' + r'')/2$ in a power series:

$$R_e(r) = R_e(z) + \sum_{k=1}^{\infty} \left(\frac{\partial^k R_e}{\partial r^k} \right)_z [(r-z)^k/k!]$$

and each matrix element of a power of r evaluated separately. The coefficients may be determined from accurate intensity data by a best least squares procedure. This will give the form of $R_e(r)$ within the radius of convergence of the power series.

39. G. Herzberg, Spectra of Diatomic Molecules, Second Ed., D. Van Nostrand Co., Inc., New York, 1961.
40. S. J. Strickler and R. A. Berg, J. Chem. Phys. 37, 814 (1962).
41. E. Rabinowitch and W. C. Wood, Trans. Faraday Soc. 32, 540 (1936).
42. P. Sulzer and K. Wieland, Helv. Phys. Acta 25, 653 (1952).
43. L. Brewer, R. A. Berg and G. Rosenblatt, J. Chem. Phys. 38, 1381 (1963). See also, R. A. Berg, Thesis, University of California Radiation Laboratory Report, UCRL-9954 (1962).
44. C. Malamond and H. Boiteux, Compt. Rend. 238, 778 (1954).

Figure Captions

- Fig. 1. Potential energy curves and examples of wavefunctions for I_2 .
- Fig. 2. Comparison between calculated and observed relative intensities for the $v' = 26$ fluorescence series. The Morse parameters used are the same as given below Table VI except for $r_e' = 3.016 \text{ \AA}$.
- Fig. 3. The variation of the internal diffraction pattern with shift in the potential. The parameter Δ measures the change of $r_e' - r_e''$ for the two potentials.

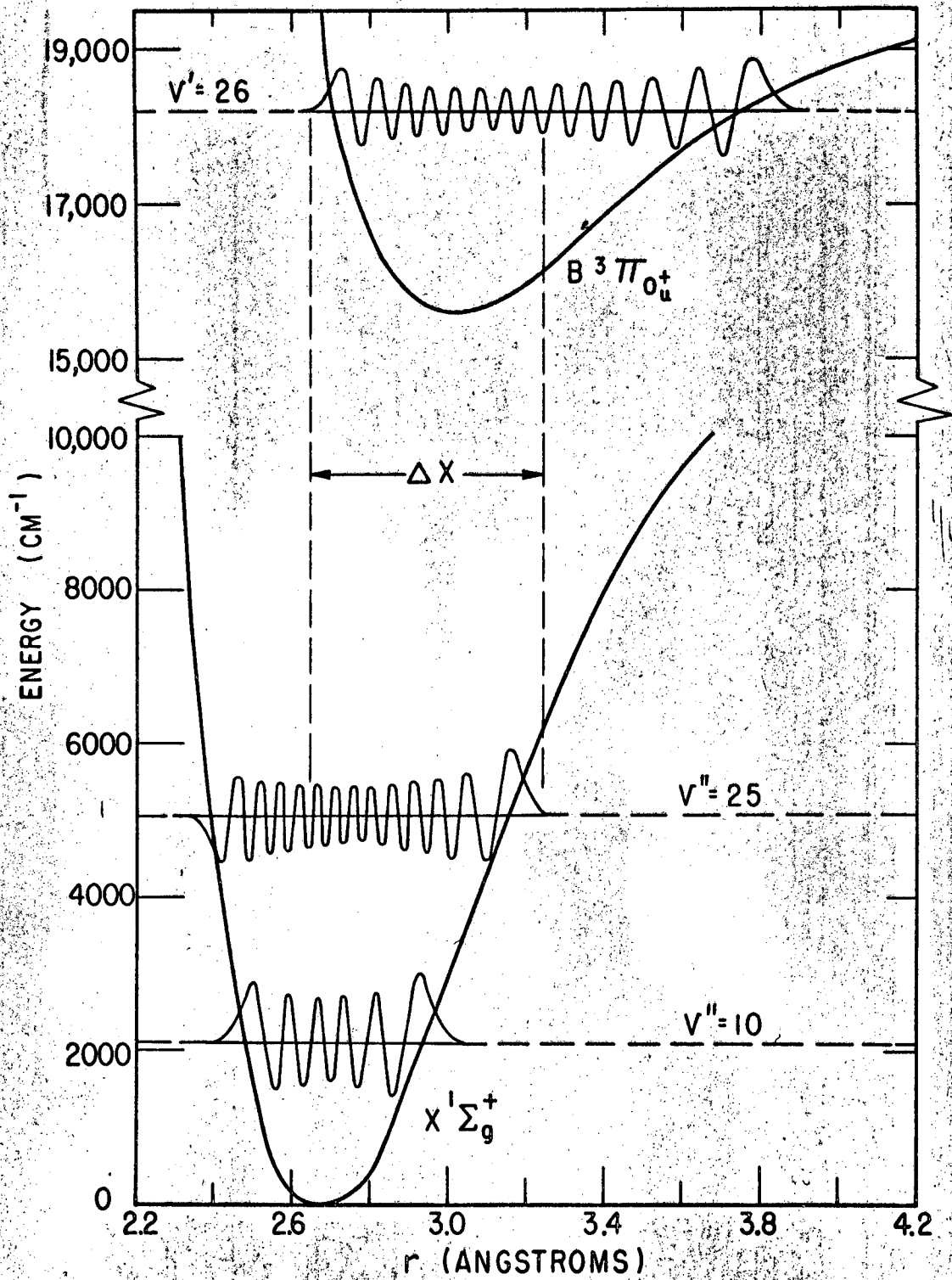


Fig. 1.

MU-31340

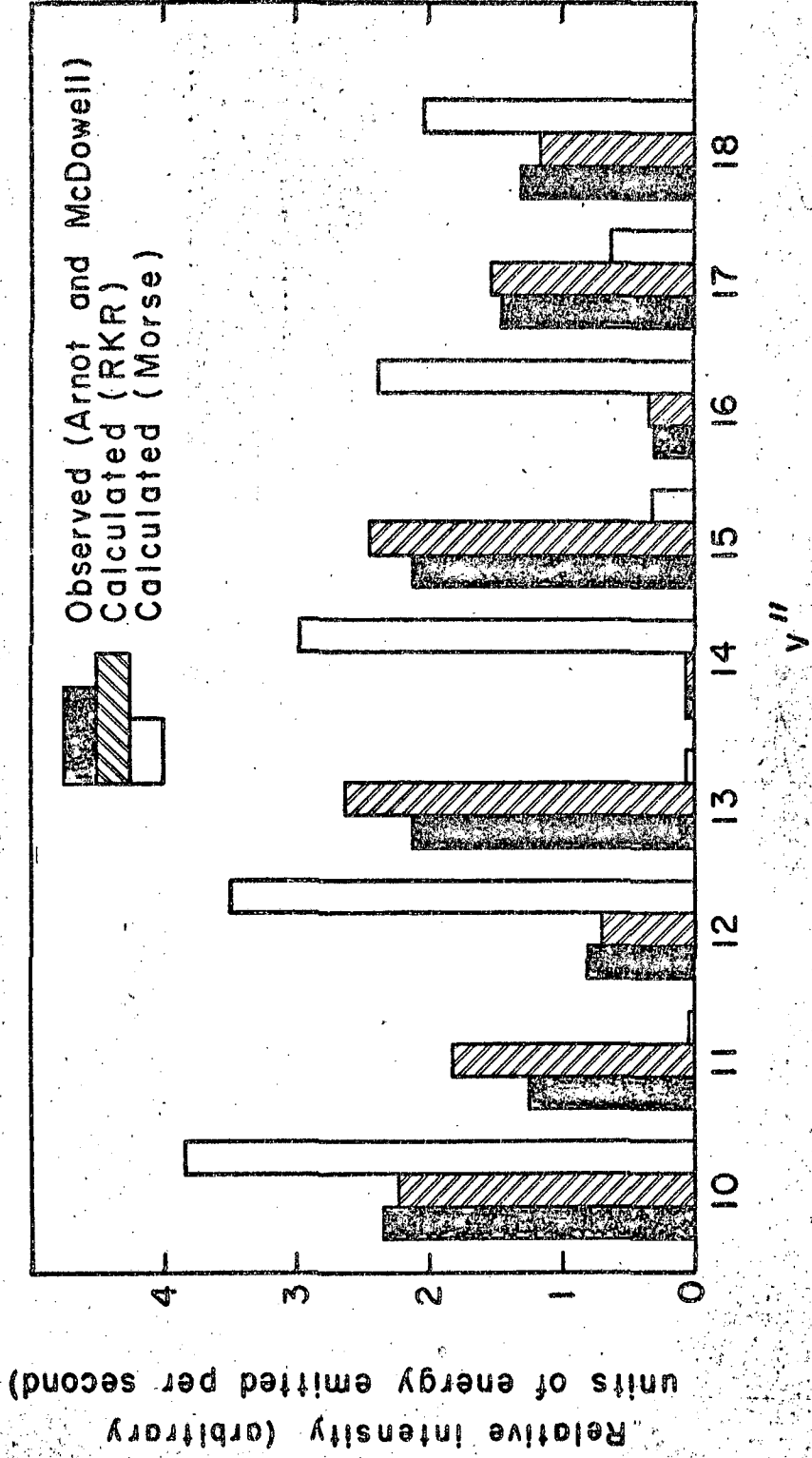
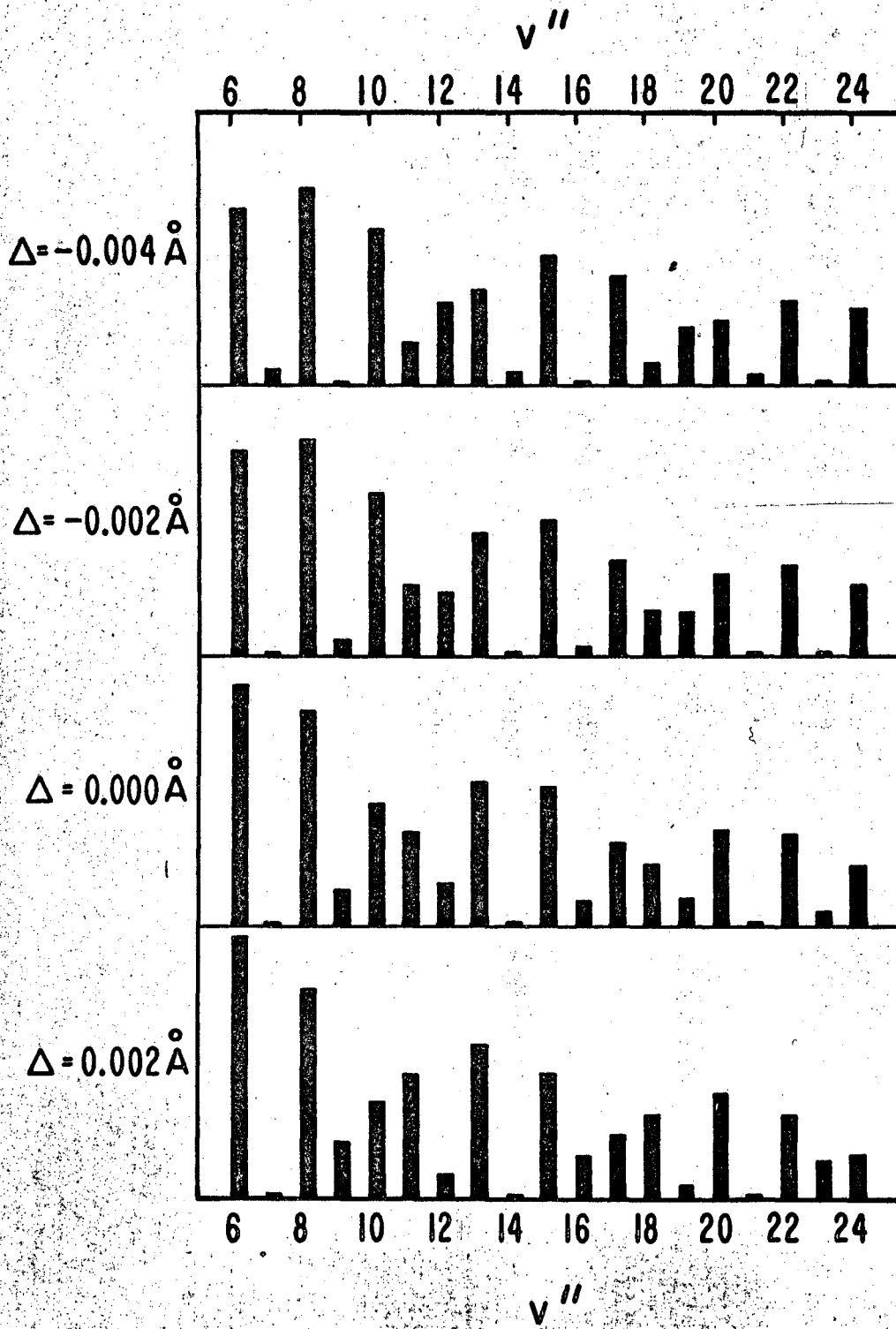


Fig. 2



MU-31341

Fig. 3.

This report was prepared as an account of Government sponsored work. Neither the United States, nor the Commission, nor any person acting on behalf of the Commission:

- A. Makes any warranty or representation, expressed or implied, with respect to the accuracy, completeness, or usefulness of the information contained in this report, or that the use of any information, apparatus, method, or process disclosed in this report may not infringe privately owned rights; or
- B. Assumes any liabilities with respect to the use of, or for damages resulting from the use of any information, apparatus, method, or process disclosed in this report.

As used in the above, "person acting on behalf of the Commission" includes any employee or contractor of the Commission, or employee of such contractor, to the extent that such employee or contractor of the Commission, or employee of such contractor prepares, disseminates, or provides access to, any information pursuant to his employment or contract with the Commission, or his employment with such contractor.